Article

Aggregation-Driven Growth of Size-Tunable Organic Nanoparticles Using Electronically Altered Conjugated Polymers

Fuke Wang, Ming-Yong Han, Khine Yi Mya, Yubo Wang, and Yee-Hing Lai

J. Am. Chem. Soc., **2005**, 127 (29), 10350-10355• DOI: 10.1021/ja0521730 • Publication Date (Web): 29 June 2005

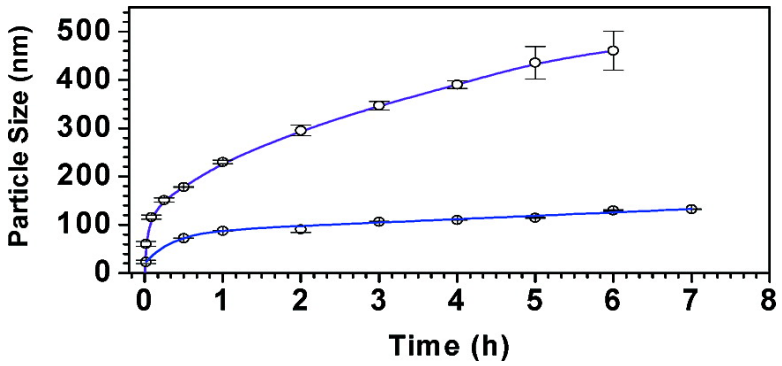

More About This Article

Additional resources and features associated with this article are available within the HTML version:

- Supporting Information
- Links to the 19 articles that cite this article, as of the time of this article download
- Access to high resolution figures
- Links to articles and content related to this article
- Copyright permission to reproduce figures and/or text from this article

View the Full Text HTML

J|A|C|S
ARTICLES
Published on Web 06/29/2005

Aggregation-Driven Growth of Size-Tunable Organic Nanoparticles Using Electronically Altered Conjugated Polymers

Fuke Wang,[†] Ming-Yong Han,*[,†,‡] Khine Yi Mya,[†] Yubo Wang,[†] and Yee-Hing Lai*[,‡]

Contribution from the Institute of Materials Research and Engineering, 3 Research Link, Singapore 117602, and the Department of Chemistry and the Division of Bioengineering, National University of Singapore, 3 Science Drive 3, Singapore 117543

Received April 5, 2005; E-mail: my-han@imre.a-star.edu.sg; biehanmy@nus.edu.sg

Abstract: A novel class of monodisperse conjugated polymer nanoparticles have been readily prepared by the facile reprecipitation of poly{1,3-bis[2-(3-alkylthienyl)]azulene} or poly{1,3-bis[2-(3-alkoxythienyl)]-azulene}. The multicomponent poly(bithiophene-*alt*-azulene) macromolecules were efficiently self-assembled into a wide range of size-tunable nanoparticles from a few tens to five hundred nanometers via the hydrophobic and π-stacking effects in the mixed chloroform/methanol solutions. Electronically altered polymer structures with different alkyl or alkoxy substitutes exhibited variable self-assembling behaviors to precisely tune the size and the optical/electronic properties of nanoparticles. A strong size dependence of continuous bathochromic absorption and significant enhanced emission were observed with the increase of particle size. A linear relationship between the absorption or fluorescence intensities and the particle size was demonstrated as well, and this is very useful to probe the intermolecular interactions and the size evolutions of conjugated polymer nanoparticles. After the size-dependent optical and electronic properties are created, they can be further optimized to improve the performance of materials prior to the use in novel organic nanodevices in a cost-effective way.

Introduction

In the past decade, inorganic and organic semiconducting materials, in particular, II−VI/III−V semiconductors and π-conjugated polymers have been extensively investigated and utilized for light-emitting devices, field-effect transistors, solar cells, lasers, and photodetectors.[1] Recent advances in the successful synthesis or fabrication of miniaturized inorganic semiconductors from micro- to nanoscale have spurred great attention due to their unique size-dependent properties[2] and novel optoelectronic and biolabeling applications.[3,4] Due to the much more structural diversity and complexity of organic molecules, the current tendentious extension of the research from nanosized inorganic to organic semiconducting materials[5,6] is expected to create a wide range of new size-dependent properties of organic nanoparticles for promising organic optoelectronic devices in a cost-effective way. A few recent reports have been initiating the investigations on the size-dependent properties of small molecular semiconductors;[7] however, there has been very little success making the size-tunable conjugated polymer

[†] Institute of Materials Research and Engineering.
[‡] National University of Singapore.

(1) (a) Ruda, H. R. *Widegap II−VI Compounds for Optoelectronic Applications*; Chapman & Hall: London, 1992. (b) Ringel, S. A. *III−V and IV−IV Materials and Processing Challenges for Highly Integrated Microelectronics and Optoelectronics*; Materials Research Society: Warrendale, PA, 1999. (c) Kraft, A.; Grimsdale, A. C.; Holmes, A. B. *Angew. Chem., Int. Ed.* **1998**, *37*, 402−428. (d) Friend, R. H. et al. *Nature* **1999**, *397*, 121−128. (e) Groenendaal, B. L.; Jonas, F.; Freitag, D.; Pielartzik, H.; Reynolds, J. R. *Adv. Mater.* **2000**, *12*, 481−494. (f) Shirota Y. *J. Mater. Chem.* **2000**, *10*, 1−25. (g) McGehee, M. D.; Heeger, A. J. *Adv. Mater.* **2000**, *12*, 1655−1668. (h) Heeger, A. J. *Angew. Chem., Int. Ed.* **2001**, *40*, 2591−2611.

(2) (a) Murray, C. B.; Norris, D. J.; Bawendi, M. G. *J. Am. Chem. Soc.* **1993**, *115*, 8706−8715. (b) Hines, M. A.; Guyot-Sionnest, P. *J. Phys. Chem.* **1996**, *100*, 468−471. (c) Peng, X.; Schlamp, M. C.; Kadavanich, A. V.; Alivisatos, A. P. *J. Am. Chem. Soc.* **1997**, *119*, 7019−7029. (d) Cao, Y. W.; Banin, U. *J. Am. Chem. Soc.* **2000**, *122*, 9692−9702. (e) Zhong, X. H.; Feng, Y. Y.; Knoll, W. Han, M. Y. *J. Am. Chem. Soc.* **2003**, *125*, 13559−13563. (f) Zhong, X. H.; Han, M. Y.; Dong, Z. L.; White, T. J.; Knoll, W. *J. Am. Chem. Soc.* **2003**, *125*, 8589−8594.

(3) (a) Colvin, V. L.; Schlamp, M. C.; Alivisatos, A. P. *Nature* **1994**, *370*, 354−357. (b) Klimov, V. I.; Mikhailovsky, A. A.; Xu, S.; Malko, A.; Hollingsworth, J. A.; Leatherdale, C. A.; Eisler, H. J.; Bawendi, M. G. *Science* **2000**, *290*, 314−317. (c) Artemyev, M. V.; Woggon, U.; Wannemacher, R.; Jaschinski, H.; Langbein, W. *Nano Lett.* **2001**, *1*, 309−314. (d) Huynh, W. U.; Dittmer, J. J.; Alivisatos, A. P. *Science* **2002**, *295*, 2425−2427. (e) Tessler, N.; Medvedev, V.; Kazes, M.; Kan, S. H.; Banin, U. *Science* **2002**, *295*, 1506−1508.

(4) (a) Chan, W. C. W.; Nie, S. M. *Science* **1998**, *281*, 2016−2018. (b) Bruchez, M.; Moronne, M.; Gin, P.; Weiss, S.; Alivisatos, A. P. *Science* **1998**, *281*, 2013−2016. (c) Han, M. Y.; Gao, X. H.; Su, J. Z.; Nie, S. M. *Nat. Biotechnol.* **2001**, *19*, 631−635. (d) Chan, W. C. W.; Maxwell, D. J.; Gao, X. H.; Bailey, R. E.; Han, M. Y.; Nie, S. M. *Curr. Opin. Biotechnol.* **2002**, *13*, 40−46. (e) Gu, H. W.; Zheng, R. K.; Zhang, X. X.; Xu, B. *J. Am Chem. Soc.* **2004**, *126*, 5664−5665.

(5) (a) An, B. K.; Kwon, S. K.; Jung, S. D.; Park, S. Y. *J. Am. Chem. Soc.* **2002**, *124*, 14410−14415. (b) Gong, X.; Milic, T.; Xu, C.; Batteas, J. D.; Drain, C. M. *J. Am. Chem. Soc.* **2002**, *124*, 14290−14291. (c) Lim, S. J.; An, B. K.; Jung, S. D.; Chung, M. A.; Park, S. Y. *Angew. Chem., Int. Ed.* **2004**, *43*, 6346−6350. (d) Christianen, P. C. M. et al. *J. Am. Chem. Soc.* **2005**, *127*, 1112−1113.

(6) (a) Xu, X. J.; Siow, K. S.; Wong, M. K.; Gan, L. M. *Langmuir* **2001**, *17*, 4519−4524. (b) Jang, J.; Oh, J. H.; Stucky, G. D. *Angew. Chem., Int. Ed.* **2002**, *41*, 4016−4019. (c) Kietzke, T.; Neher, D.; Landfester, K.; Montenegro, R.; Güntner, R.; Scherf, U. *Nat. Mater.* **2003**, *2*, 408−412. (d) Scherf, U. et al. *Adv. Mater.* **2003**, *15*, 800−804. (e) Hittinger, E.; Kokil, A.; Weder, C. *Angew. Chem., Int. Ed.* **2004**, *43*, 1808−1811. (f) Kiriy, A. et al. *Nano Lett.* **2003**, *3*, 707−712.

(7) (a) Fu, H.-B.; Yao, J. N. *J. Am. Chem. Soc.* **2001**, *123*, 1434−1439. (b) Xiao, D.; Xi, L.; Yang, W.; Fu, H.; Shuai, Z.; Fang, Y.; Yao, J. *J. Am. Chem. Soc.* **2003**, *125*, 6740−6745. (c) Xiao, D.; Yang, W.; Yao, J.; Xi, L.; Yang, X.; Shuai, Z. *J. Am. Chem. Soc.* **2004**, *126*, 15439−15444.

10.1021/ja0521730 CCC: $30.25

nanoparticles due to the difficulty of self-assembling the currently available macromolecules.[8] Therefore, it is very challenging, but more ideal, to precisely control the size-dependent properties of π-conjugated polymers for high potential applications, due to their much better processing/mechanical and readily tunable optoelectronic properties, as compared that of the small organic molecules.

The electronic and optical properties of nanosized organic semiconductors are fundamentally different from those of nanosized inorganic semiconductors. The quantum size effect of the inorganic nanoparticles becomes much stronger when the particle size is comparable to or smaller than the Bohr radius of the Wannier excitons. However, this is not expected in the organic nanoparticles because of the much smaller radius of the Frenkel excitons associated with the extended π-conjugation systems,[7,9] whose exciton size can be tuned by both the chemical alteration of the π-conjugated molecular structures and their intermolecular interactions. It is known that the inorganic nanoparticles are grown by the atom-by-atom addition via the formation of strong ionic or covalent bonds. However, organic nanoparticles are created by self-assembling the as-designed molecular building blocks via the weaker intermolecular interactions between adjacent molecules (than intramolecular covalent bonds between the atoms of a molecule), such as hydrogen bonding, $\pi-\pi$ stacking, and hydrophobic interactions, which are responsible for molecular ordering in soft materials.

Numerous attempts to generate inorganic nanoparticles have succeeded,[2] but there are only a few latter-day approaches to organic nanostructures of well-defined structure and morphology.[5−7] Conjugated polymers, usually oil soluble, were conventionally emulsified in oil-in-water droplets (physically trapped in the self-assembled cavities with a large amount of amphiphilic surfactants or stabilizers) for the formation of nanoparticles with certain size,[6a−d] but this quick process has poor control of particle morphology and intermolecular interactions for tuning their properties. Recently, due to its easy and versatile operation, the controllable aggregation/precipitation of small organic molecules in the mixed good−poor or nonpolar−polar solvents has become a popular technique for the surfactant-free preparation of the self-assembled nanoparticles.[10] Very few cases for conjugated polymers were reported as well,[6e] but no well-defined and excitonically coupled size-tunable nanoparticles have been readily prepared by the intermolecular aggregation-driven process. It is thus very important to design and synthesize new π-conjugated polymers that are capable of self-organizing into finely dispersed nanostructures for precisely tuning polymer properties and dramatically improving the performances of organic devices.

Semiconducting azulene-containing conjugated polymers were chosen and synthesized in this research due to the longstanding interest of azulene to experimental and theoretical chemists from its nonalternant aromatic structure and unusual physical properties, including its anomalous fluorescence from the second excited state to the ground state, in apparent violation of Kasha's Rule.[11] The reported polyazulenes themselves have very low solubility and more undesirable lost structural features after polymerization or subsequent oxidation.[12] Multicomponent poly{1,3-bis[2-(3-alkylthienyl)]azulene} macromolecules functionalized with different aliphatic tails can significantly improve their stability and solubility in most organic solvents.[13] In this paper, different molecular recognition motifs for intermolecular interactions, including $\pi-\pi$ stacking and hydrophobic interactions, were introduced into the functional macromolecular building blocks, which efficiently self-assemble themselves into well-defined nanoparticles for creating unique optical and electronic properties in the mixed chloroform/methanol solvents. Electronically altered poly{1,3-bis[2-(3-alkoxythienyl)]azulene} macromolecules with alkoxy side chains exhibited better control for the formation of monodisperse conjugated nanoparticles. We note that there are scarcely any previous examples of conjugated polymer nanostructures with such a high monodispersity in size without the use of templates or surfactants. We have systematically prepared a series of size-tunable nanoparticles of conjugated polymers in a diameter of a few tens to five hundred nanometers. This is an initial investigation on the size-dependent optical and electronic properties of conjugated polymer nanoparticles with the continuous bathochromic absorption and significant enhanced emission behaviors, which are drastically different from those of the molecularly dispersed macromolecular building blocks in solutions. The creation of the new optical and electronic properties of conjugated polymer nanoparticles is highly dependent on both the successful design and synthesis of the new electronically altered π-conjugated macromolecules and the better control of their excitonically coupled $\pi-\pi$ stacking organization via appropriate processing techniques. The first example of organic light-emitting devices using conjugated polymer nanoparticles has been successfully demonstrated,[6c] and it is highly expected to utilize the new size-tunable properties in the promising organic optoelectronic applications with improved performance.

Experimental Section

Materials. Anhydrous iron(III) chloride (Aldrich, 99.99%), anhydrous methanol (Mallinckrodt Chemicals, AR), and tetrahydrofuran (Aldrich, HPLC grade) were used as received. Chloroform was distilled from calcium hydride prior to use. 3-Alkylthiophene, 3-alkyl-2-bromothiophene, and 1,3-dibromoazulene were prepared as described in the literature with minor modification.[12,14]

Synthesis. A series of 1,3-bis[2-(3-alkylthienyl)]azulene and 1,3-bis[2-(3-alkoxythienyl)]azulene monomers and a series of the corresponding poly{1,3-bis[2-(3-alkylthienyl)]azulene} (**1**−**4**) (alkyl−PTA) and poly{1,3-bis[2-(3-alkoxythienyl)]azulene} (**5**, **6**) (alkoxy−PTA) were synthesized.[13] All the obtained conjugated polymers with ∼40−50 repeat units of their corresponding monomers are soluble in

(8) Hoeben, F. J. M.; Jonkheijm, P.; Meijer, E. W.; Schenning, A. P. H. J. *Chem. Rev.* **2005**, *105*, 1491−1546.
(9) (a) He, C. B.; Xiao, Y.; Huang, J. C.; Lin, T. T.; Mya, K. Y.; Zhang, X. H. *J. Am. Chem. Soc.* **2004**, *126*, 7792−7793. (b) Hu, D.; Yu, J.; Padmanaban, G.; Ramakrishnan, S.; Barbara, P. F. *Nano Lett.* **2002**, *2*, 1121−1124.
(10) (a) Horn, D.; Rieger, J. *Angew. Chem., Int. Ed.* **2001**, *40*, 4330−4361. (b) Auweter, H.; Haberkorn, H.; Heckmann, W.; Horn, D.; Luddecke, E.; Rieger, J.; Weiss, H. *Angew. Chem., Int. Ed.* **1999**, *38*, 2188−2191.
(11) (a) Churchill, M. R. *Prog. Inorg. Chem.* **1970**, *11*, 53−98. (b) Tetreault, N.; Muthyala, R. S.; Liu, R. S. H.; Steer, R. P. *J. Phys. Chem. A* **1999**, *103*, 2524−2531. (c) Liu, R. S. H.; Muthyala, R. S.; Wang, X. S.; Asato, A. E. *Org. Lett.* **2000**, *2*, 269−271. (d) Lou, Y.; Chang, J.; Jorgensen, J.; Lemal, D. M. *J. Am. Chem. Soc.* **2002**, *124*, 15302−15307. (e) Shevyakov, S. V.; Li, H.; Muthyala, R. S.; Asato, A. E.; Croney, J. C.; Jameson, D. M.; Liu, R. S. H. *J. Phys. Chem. A* **2003**, *107*, 3295−3299.
(12) (a) Wang, F. K.; Lai, Y. H.; Kocherginsky, N. M.; Kosteski, Y. Y. *Org. Lett.* **2003**, *5*, 995−998. (b) Porsch, M.; Sigl-Seifert, G.; Daub, J. *Adv. Mater.* **1997**, *9*, 635−639.
(13) (a) Wang, F. K.; Lai, Y. H.; Han, M. Y. *Macromolecules* **2004**, *37*, 3222−3230. (b) Wang, F. K.; Lai, Y. H. *Macromolecules* **2003**, *36*, 536−538. (c) Wang, F. K.; Lai, Y. H.; Han, M. Y. *Org. Lett.* **2003**, *5*, 4791−4794.
(14) McCullough, R. D.; Lowe, R. D.; Jayaraman, M.; Anderson, D. L. *J. Org. Chem.* **1993**, *58*, 904−912.

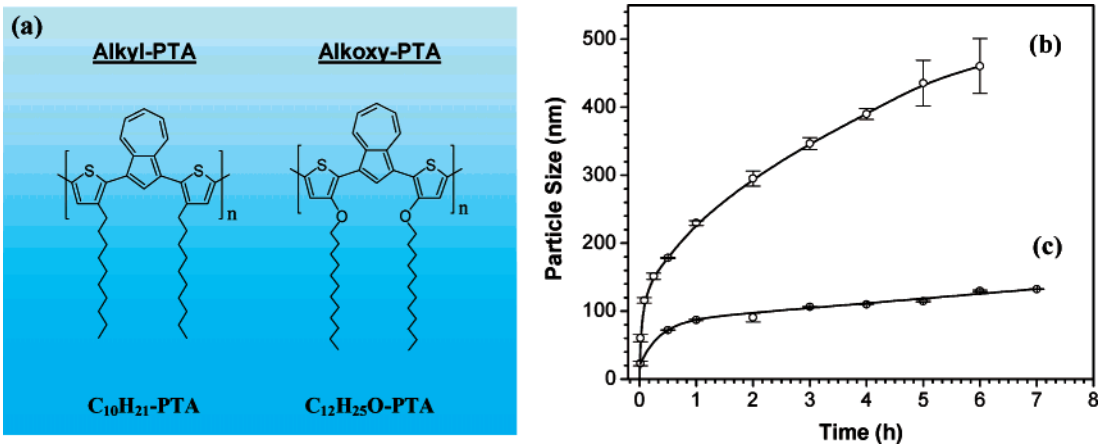

Figure 1. (a) Chemical structures of poly{1,3-bis[2-(3-*n*-decylthienyl)]azulene} ($C_{10}H_{21}$−PTA, M_n = 25 800, repeat number of monomers = ∼45) and poly{1,3-bis[2-(3-*n*-dodecoxythienyl)]azulene} ($C_{12}H_{25}O$−PTA, M_n = 35 100, repeat number of monomers = ∼48). Time-dependent size evolutions of conjugated polymer nanoparticles in the 1:1 mixed chloroform/methanol solutions containing (b) 1 × 10^{-5} M $C_{10}H_{21}$−PTA and (c) 1 × 10^{-5} M $C_{12}H_{25}O$−PTA, respectively.

chloroform, tetrahydrofuran, and toluene. Model compounds 1,3-bis(2-thienyl)azulene (**7**), 1,3-bis[2-(3-methylthienyl)]azulene (**8**), 1,3-bis[2-(3-methoxythienyl)]azulene (**9**), and 1,3-bis[2-(3-*n*-hexoxythienyl)]azulene (**10**) were also prepared from the Grignard coupling of 1,3-dibromoazulene with 2-bromothiophene, 2-bromo-3-methylthiophene, 2-bromo-3-methoxythiophene, and 2-bromo-3-hexoxythiophene, respectively.[13]

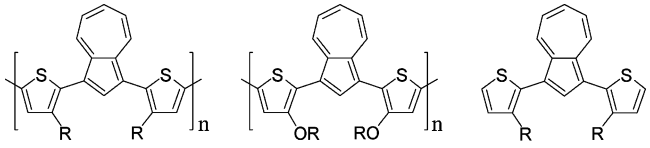

1, R = C_4H_9
2, R = C_7H_{15}
3, R = $C_{10}H_{21}$
4, R = $C_{14}H_{29}$
5, R = C_6H_{13}
6, R = $C_{12}H_{25}$
7, R = H
8, R = CH_3
9, R = OCH_3
10, R=OC_6H_{13}

Preparation of Conjugated Polymer Nanoparticles. Conjugated polymer nanoparticles of alkyl−PTA and alkoxy−PTA were prepared by vigorously mixing a 2 × 10^{-5} M polymer solution in chloroform with methanol at an equal volume ratio. The mixed solution was left at room temperature, and the aliquots of the solution were taken at different time intervals for characterization. The SEM samples were prepared by dispersing the suspension solution of polymer nanoparticles on gold-coated glass slides followed by quickly removing the mixed solvents with a piece of filter paper.

Characterization. Number-average molecular weights (M_n) were determined by size-exclusion chromatography (SEC) equipped with an HPLC pump and a UV−vis detector. UV−visible absorption spectra were recorded with a Hewlett-Packard 8453 diode-array spectrophotometer. Photoluminescence spectra were performed on a LS 55 PerkinElmer luminescence spectrophotometer. Size and morphology of conjugated polymer nanoparticles were examined with a JEOL JSM 6700 field-emission scanning electron microscope (SEM). Size-evolution of conjugated polymer nanoparticles was measured at 25 °C on a Brookhaven light-scattering instrument equipped with a BI-200SM multiangle goniometer and a 35 mW He−Ne laser (vertically polarized 632.8 nm light). The sample cell containing 2 × 10^{-5} M polymer solution in chloroform was mounted in a temperature-controlled, refractive index matched bath, which is filled with decahydronaphthalene. An equal volume of methanol (1:1 ratio) was then mixed into the sample cell followed by the dynamic light-scattering (DLS) measurement at different time intervals. The refractive index and the viscosity of the mixed solvents were used according to the literature values.[15]

Results and Discussions

The molecularly dispersed solution of $C_{10}H_{21}$−PTA or $C_{12}H_{25}O$−PTA (Figure 1a) in chloroform is a very transparent, yellowish solution. After mixing it with a poor solvent (methanol), the sudden change of environment and the formation of supersaturated polymer solution led to the subsequent growth of conjugated polymer nanoparticles in the mixed solvents. The time-dependent size evolutions of $C_{10}H_{21}$−PTA and $C_{12}H_{25}O$−PTA nanoparticles were monitored by the DLS in the 1:1 mixed solution of chloroform and methanol, as revealed in Figure 1b,c, respectively. In the first minute, the particle size of $C_{10}H_{21}$−PTA was reached at ∼60 nm, and the particle size of $C_{12}H_{25}O$−PTA was only ∼23 nm. In the following 4 h, the resulting uniform $C_{10}H_{21}$−PTA nanoparticles grew continuously from ∼60 to 400 nm in diameter. After that, much larger nanoparticles (up to ∼500 nm) with a wider size distribution were formed. However, the resulting $C_{12}H_{25}O$−PTA nanoparticles had a very narrow size distribution during the entire growth process. Their particle size was increased from ∼30 to 100 nm in the first 2 h. After that, the particle size was retained with a small increase from ∼100 to 130 nm within the following 5 h. In comparison, the particle size of $C_{10}H_{21}$−PTA was increased dramatically with increasing time, while the particle size of $C_{12}H_{25}O$−PTA was increased gradually. The similar size evolutions of uniform conjugated polymer nanoparticles were verified by the SEM observations in Figures 2 and 3. The size of spherical $C_{10}H_{21}$−PTA nanoparticles was increased from ∼60, 120, 240, to 400 nm with the increase of time from 1, 10, 60, to 240 min, respectively. The sizes of spherical $C_{12}H_{25}O$−PTA nanoparticles of ∼30 and 100 nm were also obtained at the reaction time of 1 and 120 min, respectively. It is noted that 2 × 10^{-5} M $C_{10}H_{21}$−PTA in chloroform was an optimized concentration for the size-tunable preparation of $C_{10}H_{21}$−PTA nanoparticles in the 1:1 mixed chloroform/methanol solvents. Lower polymer concentration did not lead to the formation of

(15) Marcus, Y. *Solvent Mixtures, Properties and Selective Solvation*; Marcel Dekker: New York, 2002.

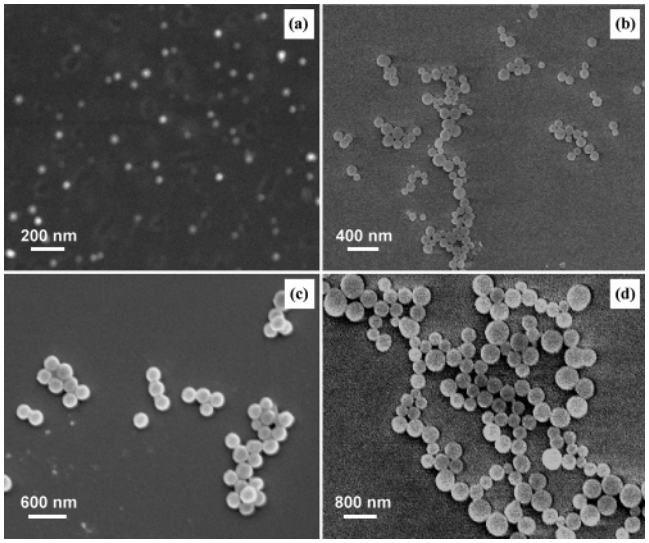

Figure 2. SEM images of $C_{10}H_{21}$−PTA nanoparticles prepared in the 1:1 mixed chloroform/methanol solvents in the time course of (a) 1 min, (b) 10 min, (c) 60 min, and (d) 240 min.

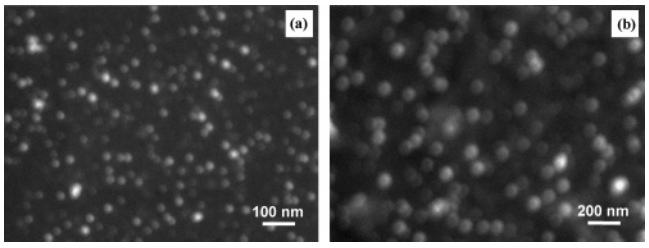

Figure 3. SEM images of $C_{12}H_{25}O$−PTA nanoparticles prepared in the 1:1 mixed chloroform/methanol solvents in the time course of (a) 1 min and (b) 120 min.

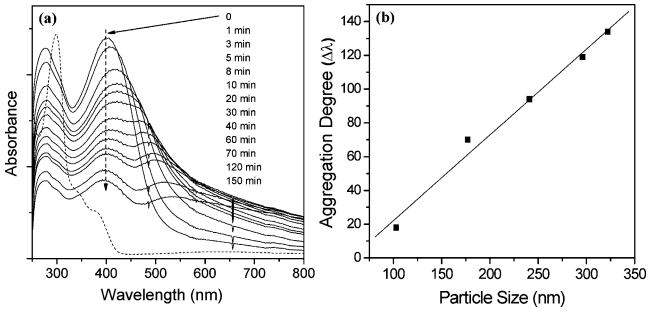

Figure 4. (a) Time-dependent evolution of the absorption spectra of $C_{10}H_{21}$−PTA nanoparticles in the time course of the first 150 min after mixing an equal volume of methanol with the chloroform solution of molecularly dissolved $C_{10}H_{21}$−PTA. The absorption spectrum of the molecularly dispersed $C_{10}H_{21}$−PTA in chloroform was recorded when time is zero. (b) Time-dependent aggregation degree as a function of the size of $C_{10}H_{21}$−PTA nanoparticles. For comparison, the absorption spectrum of the corresponding monomer, 1,3-bis[2-(3-*n*-decylthienyl)]azulene ($C_{10}H_{21}$−TA), in chloroform is also shown in (a) (dashed line), and the strong absorption of $C_{10}H_{21}$−PTA at ∼400 nm was due to the polymerization of $C_{10}H_{21}$−TA to extend the delocalization of the π-conjugation system.

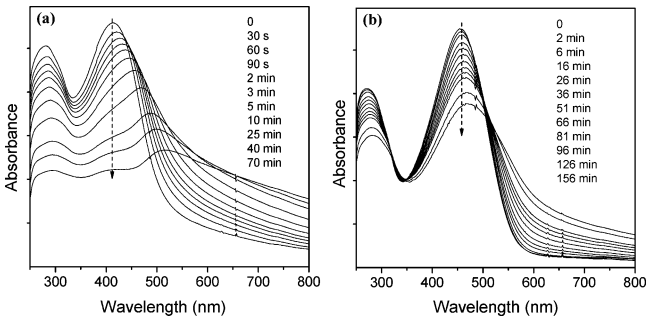

Figure 5. Aggregation behavior of (a) $C_{14}H_{29}$−PTA and (b) $C_{12}H_{25}O$−PTA with lengthy alkyl and alkoxy substitutes, respectively, in the 1:1 mixed solution of chloroform and methanol.

$C_{10}H_{21}$−PTA nanoparticles, and higher polymer concentration, such as $>10^{-3}$ M, led to the significantly enhanced formation rate of larger polymer nanoparticles with wider size distribution. Meanwhile, 1:1 mixed chloroform/ethanol and dichloromethane/ethanol solvents were also used, and the resulting particles were not very uniform.

To correlate with the DLS and SEM observations, the kinetic formation process of $C_{10}H_{21}$−PTA nanoparticles in the 1:1 mixed solvent of chloroform and methanol was further demonstrated by the spectroscopic investigations, as revealed in Figure 4a. After mixing methanol into the polymer solution in chloroform, the maximum absorption wavelength (λ_{max}) of the $C_{10}H_{21}$−PTA backbones at ∼400 nm remained essentially unchanged, and the maximum absorption intensity was reduced gradually. However, a newly formed peak was also clearly shown in the time-dependent evolution process of the absorption spectra of $C_{10}H_{21}$−PTA nanoparticles due to the intermolecular interaction/aggregation between $C_{10}H_{21}$−PTA macromolecules for the formation of conjugated polymer nanoparticles. The newly formed peak in the range of 420−530 nm was red shifted continuously due to the consecutive aggregation-driven growth of conjugated polymer nanoparticles from small to large to extend the delocalization of the π-electron conjugation system. Meanwhile, the maximum absorption intensity of the $C_{10}H_{21}$−PTA backbones at ∼400 nm was also continually reduced due to the continuous consumption of free $C_{10}H_{21}$−PTA macromolecules in the mixed solvents. As shown in Figure 4b, the position of the newly formed peak in the range of 420−530 nm is strongly associated with the size of polymer nanoparticles. The red shift value ($\Delta\lambda$) between the λ_{max} for the newly formed peak and λ_{max} at ∼400 nm for the free macromolecules in solution is used to express the aggregation degree of $C_{10}H_{21}$−PTA. A linear relationship between the $\Delta\lambda$ and the size of $C_{10}H_{21}$−PTA nanoparticles confirmed the continuous seeded growth of nanoparticles because there are not much smaller nanoparticles formed in the same reaction solution as observed by SEM.

The aggregation-driven growth of alkyl−PTA nanoparticles is weakly affected in the mixed chloroform/methanol solvents by using the different chain lengths of alkyl−PTA. In comparison between Figures 4a and 5a, the intermolecular aggregation-based consumption of free macromolecules with the longer alkyl chains is only a little faster due to the relatively stronger hydrophobic interactions between neighboring longer alkyl chains, and the shorter chain length only led to a slower growth of nanoparticles. The similar aggregation behavior was attributed to the weak influence of alkyl substitution on its electronic structure of conjugated polymer backbones, which is also indicated by the identical λ_{max} at ∼400 nm for all the alkyl−PTA with different lengths of alkyl chains (C_4H_9−, C_7H_{15}−, $C_{10}H_{21}$−, and $C_{14}H_{29}$−) in chloroform. To the contrary of the alkyl substitution of poly(bithiophene-*alt*-azulene), the alkoxy substitutes have a large influence on its electronic properties and further the formation process of nanoparticles. As shown

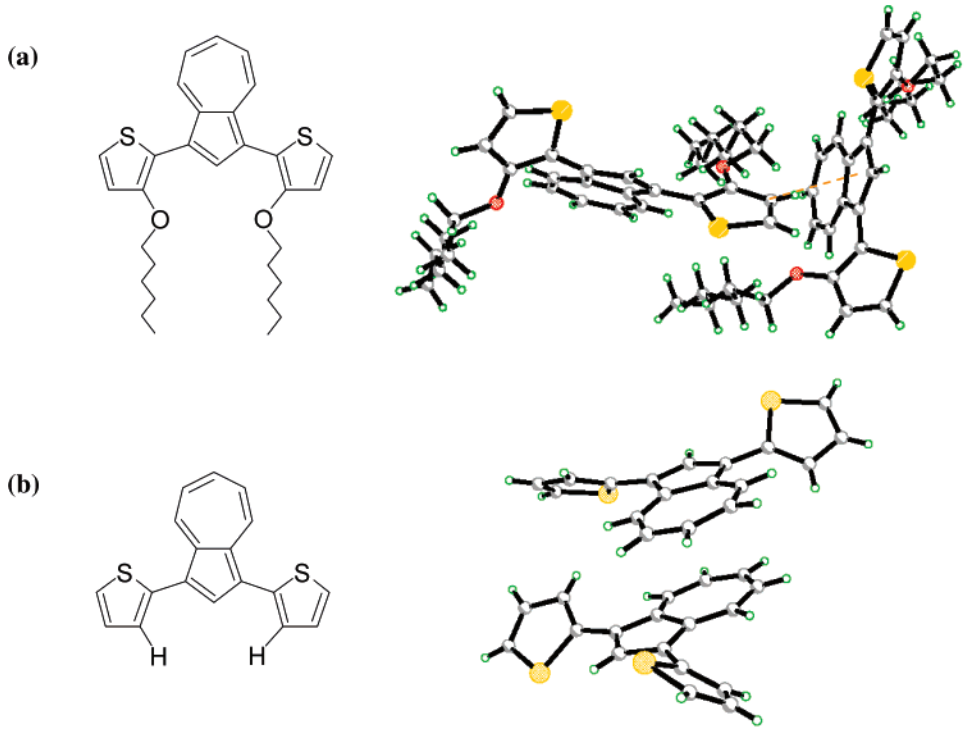

Figure 6. ORTEP drawings of (a) 1,3-bis[2-(3-*n*-hexoxythienyl)]azulene and (b) 1,3-bis(2-thienyl)azulene.

in Figures 4a and 5, the large red shift of ~65 nm in the λ_{max} of $C_{12}H_{25}O-$PTA as compared to that of $C_{10}H_{21}-$PTA in chloroform indicates an electron donation of alkoxy groups ($C_{12}H_{25}O-$) to the conjugated polymer backbones that is stronger than that of the alkyl groups ($C_{10}H_{21}-$). As there is no strong hydrogen bonding between conjugated backbones, the real driving force for conjugative aggregation is believed to be associated with the $\pi-\pi$ stacking of conjugated polymer backbones in addition to the hydrophobic interactions between neighboring side chains. As compared to the $C_{10}H_{21}-$PTA, this stronger $\pi-\pi$ interaction between neighboring $C_{12}H_{25}O-$PTA molecules may facilitate the quick nucleation and the subsequent formation of a large number of smaller nanoparticles after mixing with the poor solvent, methanol. The fast consumption of free macromolecules (the quickly reduced concentration) in solution further limits the growth of the smaller nanoparticles into larger ones. In the time course of 150 min, the obtained smaller polymer nanoparticles resulted in the smaller red shift due to the smaller aggregation degree of conjugated polymers, as shown in Figure 5b. Free $C_{12}H_{25}O-$PTA macromolecules were almost depleted after 150 min because only very shallow color remained in solution after high-speed centrifugation, indicating the fast and dominant formation of smaller nanoparticles with a small red shift in the maximum absorption wavelength, which is similar to that of the smaller $C_{10}H_{21}-$PTA nanoparticles at their early period of growth, as shown in Figure 4a.

Although the spectroscopic investigations provided the information of intermolecular interactions in the resulting noncrystalline nanoparticles of alkyl−PTA and alkoxy−PTA, a better understanding of the molecular stacking of conjugated polymer backbones could be obtained from the crystallographic structures of their corresponding monomers. However, most of the monomers with longer side chain, such as C_4H_9-, $C_7H_{15}-$, $C_{10}H_{21}-$, $C_{14}H_{29}-$, and $C_{12}H_{25}O-$TA, are liquid at room temperature. Luckily, 1,3-bis[2-(3-*n*-hexoxythienyl)]azulene ($C_6H_{13}O-$TA) is solid at room temperature and was crystallized successfully in the mixed solution of dichloromethane and hexane. The ORTEP drawing of the $C_6H_{13}O-$TA crystallographic structure (Supporting Information) in Figure 6a shows its favorable molecular configuration with a T-shaped $\pi-\pi$ interaction between the thiophene moiety and the seven-membered ring of azulene, which are from the neighboring two macromolecular backbones, respectively. The T-shaped $\pi-\pi$ interaction is also favored in some other π-conjugated systems, like benzene dimers, and could be accounted by the aggregation-driven growth of conjugated polymer nanoparticles.[16] The nearest distance from the C_{13} of thiophene to the five-membered ring of azulene is 3.67 Å, as indicated in Figure 6a. As expected, the ORTEP drawing of the 1,3-bis(2-thienyl)azulene crystallographic structure (Supporting Information) in Figure 6b also shows that the intermolecular dipolar interaction between two neighboring azulene molecules (with a smaller face-to-face distance of 3.452 Å) is due to the larger intrinsic dipole moment (1.0 D) of azulene (with a electron-rich five-membered ring and a electron-deficient seven-membered ring).[11] The intermolecular dipolar interaction effect between neighboring azulene molecules in $C_6H_{13}O-$TA crystal is weakened by the bulky alkoxy chains and their electronic donating properties. There fore, the bathochromic shift of the conjugated polymer nanoparticles with the increase of the particle size was mainly attributed to the $\pi-\pi$ interactions between the thiophene and azulene moieties from the closely stacked, neighboring polymer backbones because of the gradually increased excitonic coupling

(16) (a) Sinnokrot, M. O.; Valeev, E. F.; Sherrill, C. D. *J. Am. Chem. Soc.* **2002**, *124*, 10887−10893. (b) Cozzi, F.; Annunziata, R.; Benaglia, M.; Cinquini, M.; Raimondi, L.; Baldridge, K. K.; Siegel, J. S. *Org. Biomol. Chem.* **2003**, *1*, 157−162.

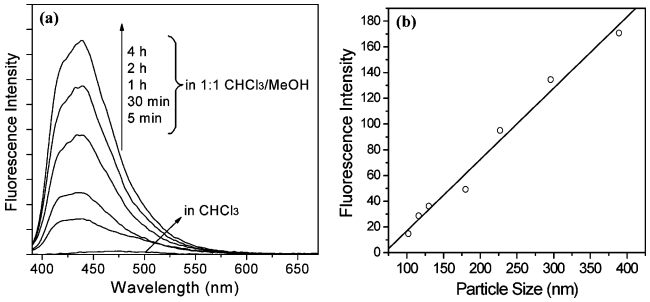

Figure 7. (a) Fluorescence spectra of $C_{10}H_{21}$−PTA nanoparticles in the 1:1 mixed solution of chloroform and methanol at variable time intervals, excited at 370 nm. (b) Fluorescence intensity of $C_{10}H_{21}$−PTA nanoparticles as a function of particle size. The maximum absorption wavelength of $C_{10}H_{21}$−PTA nanoparticles (~400 nm) was not chosen as the excitation wavelength due to the small stock shift.

effect and the more extended π-electron delocalization among more conjugated macromolecules. The red shifted λ_{max} arises from the $\pi-\pi$ orbital overlap of the closely stacked/aggregated polymer backbones in nanoparticles and is similar to the previous observations of the aggregation states of small organic molecules.[7]

The nonfluorescence of molecularly dispersed alkyl−PTA and alkoxy−PTA in chloroform is attributed to the large torsional angles and high rotational energy barriers between the neighboring chromophores. The crystallographic data show that the dihedral angles between the five-membered ring of azulene and the two adjacent thiophene rings are 40 and 44° in $C_6H_{13}O$−TA, respectively (due to the steric effect of the bulky seven-membered ring of azulene). In the alkyl−PTA and alkoxy−PTA, the active intramolecular rotation of the peripheral thiophene rings around the axes of the single bonds linked to the central azulene ring and the free rotation of the alkyl side chains in solution may effectively annihilate the excitons through increasing the nonradiative decay rates, predominately by $S_2 \rightarrow S_1$ internal conversion of azulene.[11] However, for instance, a dramatic change of fluorescence intensity of $C_{10}H_{21}$−PTA nanoparticles was observed from the virtually no fluorescent polymers in chloroform to their luminescent polymeric nanoparticles in the mixed chloroform/methanol solvents. The aggregation-induced enhanced emission is caused by the restricted intramolecular rotation of the bulky alkyl groups and the restricted torsional motions of the molecules between the central azulene ring and the peripheral thiophene moieties in their aggregate form, which lead to the deactivation of nonradiative decay.[17] The time-dependent fluorescence spectra of $C_{10}H_{21}$−PTA nanoparticles were investigated in the 1:1 mixed solvents of chloroform and methanol, as shown in Figure 7a. The fluorescence intensity increased significantly with the increase of the particle size, and a linear relationship was further analyzed between the particle size and the fluorescence intensity of $C_{10}H_{21}$−PTA nanoparticles, exhibiting unique size-dependent emission properties (Figure 7b). That is to say that the smaller $C_{10}H_{21}$−PTA nanoparticles have weak fluorescence and the larger $C_{10}H_{21}$−PTA nanoparticles have enhanced fluorescence. This aggregation-induced emission from conjugated polymer nanoparticles is further depicted by the fluorescence intensity of other alkyl−PTA nanoparticles; however, only weak fluorescence was observed due to the exclusive formation of smaller $C_{12}H_{25}O$−PTA nanoparticles. In comparison with $C_{10}H_{21}$−PTA nanoparticles, $C_{10}H_{21}$−PTA films were also prepared by drying 2×10^{-5} M $C_{10}H_{21}$−PTA in chloroform on glass substrate. The obtained $C_{10}H_{21}$−PTA film only showed a very broad absorption spectrum due to much more excitonically coupled macromolecules in polymer film than that in polymer nanoparticles and a weak PL spectrum due to the strong re-absorption by the film itself, which lack the information of intermolecular interaction or aggregation.

(17) (a) Chen, J. W.; Xu, B.; Ouyang, X. Y.; Tang, B. Z.; Cao, Y. *J. Phys. Chem. A* **2004**, *108*, 7522−7526. (b) Ren, Y.; Lam, J. W. Y.; Dong, Y.; Tang, B. Z.; Wong, K. S. *J. Phys. Chem. B* **2005**, *109*, 1135−1140.

Conclusion

A new class of monodisperse nanoparticles of conjugated polymers has been readily prepared, and their particle size was continuously tuned over a wide range from a few tens to five hundred nanometers, which is similar to the as-reported size evolution process of size-tunable inorganic nanoparticles, such as CdSe. In this research, the multicomponent alkyl−PTA and alkoxy−PTA were efficiently self-assembled at nanoscale by the hydrophobic and π-stacking effects in the mixed chloroform/methanol solvents. The electronically tailored electronic structures of poly(bithiophene-*alt*-azulene) with different alkyl and alkoxy substitutes exhibited a strong influence on the self-assembling behavior for controlling the formation and the properties of size-tunable nanoparticles of conjugated polymers. A strong size dependence of continuous bathochromic absorption and significant enhanced emission (nonemissive, molecularly dispersed conjugated polymers were aggregated into luminescent organic nanoparticles) with the increase of particle size were demonstrated. We envision that the successful preparation of size-tunable organic nanoparticles can facilitate the creation of a wide range of new size-dependent optical and electronic properties, which can be further optimized to improve performance of materials prior to the use in novel organic nanodevices in a cost-effective way. This unique linear relationship between the fluorescence (or absorption) intensity and the particle size can be used as a sensitive probe to study the intermolecular interactions and the size-evolution of conjugated polymer nanoparticles.

Acknowledgment. This work was financially supported by the National University of Singapore and the Institute of Materials Research and Engineering.

Supporting Information Available: Crystallographic data of 1,3-bis[2-(3-*n*-hexoxythienyl)]azulene and 1,3-bis(2-thienyl)-azulene in CIF format. This material is available free of charge via the Internet at http://pubs.acs.org.

JA0521730